

Luminescence processes in amorphous hydrogenated silicon-nitride nanometric multilayers

F. Giorgis* and C. F. Pirri

INFN and Physics Department, Polytechnic of Torino, C.so Duca degli Abruzzi 24, 10129 Torino, Italy

C. Vinegoni and L. Pavesi

INFN and Physics Department, University of Trento, Via Sommarive 14, 38050 Povo, Italy

(Received 27 October 1998; revised manuscript received 28 April 1999)

Radiative recombinations in amorphous $\text{Si}_{1-x}\text{N}_x\text{:H}$ -based nanometric multilayer structures have been studied by stationary and time-resolved photoluminescence measurements at room temperature. Such structures show higher photoluminescence efficiency than reference bulk amorphous silicon nitride films. The enhancement is attributed to the localization of electron-hole pairs induced by the multilayer structure. Fast monomolecular recombination processes are shown, with lifetimes dependent on the emission energy. Analysis of photoluminescence and absorption spectra shows a low density of defects and no intermixing at the multilayer heterointerfaces. Such features open the potential for the investigated structures to function as fast optoelectronic devices. [S0163-1829(99)13635-X]

In the last decade, many efforts have been devoted to the study of nanometric multilayers based on amorphous silicon and its alloys, like $a\text{-SiN}$ - and $a\text{-SiC}$ -based systems. Amorphous nanometric multilayers are very promising for optoelectronics applications, such as solar cells,¹ thin-film transistors,² optical sensors,³ and light-emitting devices (LEDS).⁴ With regard to $a\text{-Si}_{1-x}\text{N}_x\text{:H}$ alloys, their optical band gap increases monotonically with x having values from 1.9 to 5 eV,⁵ an energy range not fully covered by other Si-based amorphous alloys such as $a\text{-SiC:H}$. This renders the $a\text{-Si}_{1-x}\text{N}_x\text{:H}$ system very appealing for the realization of multilayers. In addition, $a\text{-Si}_{1-x}\text{N}_x\text{:H}$ alloys show high radiative efficiency.⁶ Such features indicate that compositional periodic multilayers based on the $a\text{-Si}_{1-x}\text{N}_x\text{:H}$ system may be a promising structure for LED applications. It is worth noting that in previous works on amorphous multilayers, the active layers consisted of low optical gap materials (where low optical gap means an energy gap below 2 eV). In this paper, we analyze the optical and radiative performance of structures composed entirely of wide-band-gap $a\text{-Si}_{1-x}\text{N}_x\text{:H}$ -based nanometric multilayers. Such structures yield an emission energy tunable from the near-infrared to the visible range.

The $a\text{-Si}_{1-x}\text{N}_x\text{:H}$ multilayers were deposited by a multi-chamber rf 13.56-MHz plasma-enhanced chemical vapor deposition system⁷ with $\text{SiH}_4+\text{NH}_3+\text{H}_2$ gas mixture. All the samples were deposited at a substrate temperature of 220 °C, pressure of 0.8–0.9 mbar, a rf power of 4 W, an electrode area of 144 cm², an electrode distance of 20 mm, and a total gas flow in the range 75–110 sccm. At each heterointerface, the rf discharge was interrupted and the deposition chamber was evacuated. To achieve a sharp interface the rf plasma off-interval was 10 s, a much longer time than that needed for the growth of an atomic monolayer. In fact, hydrogen dilution of SiH_4+NH_3 gas mixtures was employed to reduce the deposition rate to values of around 0.6–0.7 Å/s,⁵ so as to improve the thickness control of the single layers.

The investigated structures are formed by periodic repetitions of $a\text{-Si}_{0.6}\text{N}_{0.4}\text{:H}$ with an optical gap of 2.6 eV (referred

to in the following as the well layer) and of $a\text{-Si}_3\text{N}_4\text{:H}$ with an optical gap of 5 eV (referred to as the barrier layer). Here, the optical gap is defined as the energy at which the absorption coefficient is equal to 10^4 cm^{-1} (E_{04}). The thickness of the well and barrier layers ranges from 5 to 100 Å. The compositional periodicity has been verified by secondary-ion-mass spectrometry⁸ and cross-section transmission electron microscopy.

Characterization by optical absorption at energies below the optical gap of the multilayers was performed by photothermal deflection spectroscopy (PDS) in order to extract information about defects located at the surface and at the various heterointerfaces. Continuous-wave photoluminescence measurements (cw PL) were performed at room temperature in a back-scattering geometry using a double monochromator, an Ar⁺ laser line at 2.71 eV with 500 mW/cm², a cooled photomultiplier equipped for photon-counting technique, or a Si photodiode (used for longer wavelengths) whose signal was processed by a digital lock-in amplifier. Time-resolved photoluminescence measurements (TRPL) were performed at room temperature using a mode-locked frequency-doubled Ti:sapphire laser as pulsed excitation source (pulse duration 2 ps, wavelength 390 nm, repetition frequency 4 MHz, and a mean power of 50 mW/cm²). A single monochromator coupled to a streak camera directly interfaced to a computer was used for the recording of two-dimensional (time and wavelength) luminescence maps.

Figure 1 shows the room-temperature cw PL spectra of the multilayer samples and of a reference bulk $a\text{-Si}_{0.6}\text{N}_{0.4}\text{:H}$ sample 7500 Å thick; the spectra are normalized by the factor $[1-R][1-\exp(-\alpha d)]$, where R , α , and d are the reflectance at 2.71 eV, the absorption coefficient at 2.71 eV, and the thickness of the absorbent material, respectively. This normalization takes into account the loss of the impinging excitation light due to the reflectivity and transmittance of the samples. The multilayer samples show a stronger emission with respect to that of the bulk. In addition, some systematic trends as a function of barrier and well thicknesses are observed. In Fig. 1(a), samples with 30 periods and with

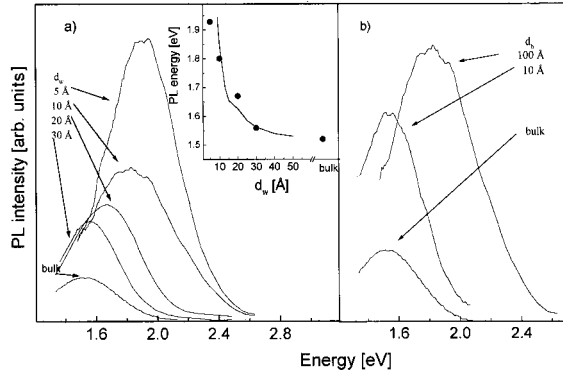


FIG. 1. Room-temperature photoluminescence spectra of multilayer samples whose parameters are (a) a fixed barrier thickness of 100 Å and different well thicknesses as indicated, and (b) a fixed well thickness of 10 Å and different barrier thicknesses as indicated. As a reference the photoluminescence spectra of an $a\text{-Si}_{0.6}\text{N}_{0.4}:\text{H}$ thin film is reported and indicated as bulk. The inset shows E_L vs well thickness (● symbols), compared with the blueshift predicted by Eq. (3) (continuous line).

the same barrier thicknesses ($d_b = 100$ Å) but different well thickness ($d_w = 5, 10,$ and 30 Å) are compared. As the well thickness decreases, a blueshift of the emission peak (E_L) and a strong increase of the radiative efficiency are observed. In Fig. 1(b) the PL emission of samples with the same well thickness ($d_w = 10$ Å) but different barrier thicknesses ($d_b = 10$ and 100 Å) are compared. When d_b decreases, the PL intensity decreases.

In the past, semiclassical⁹ or quantum confinement^{10,11} models have been proposed to explain the blueshift and the increase of emission intensity when the well thickness decreases. Following the semiclassical model, the PL intensity increase is due to the reduction of nonradiative recombination center density in the region spanned by the e - h pairs, while the blueshift is due to the concurrent reduction of the deep tail states. The second model claims that quantum confinement occurs for the e - h pairs in the well layers which opens the band gap (blueshift) and increases the energy difference between band states and nonradiative mid gap states which, in turn, reduces the capture rate of e - h pairs (luminescence intensity increases). In particular, very recent tight-binding calculations concerning amorphous silicon layers attribute the observed blueshift of the luminescence to quantum confinement for a layer thickness below 30 Å.¹²

By analyzing the cw PL results of our structures, the increase of PL efficiency can be ascribed to a strong spatial localization of electron-hole pairs in the well layers which adds to the disorder induced localization typical of amorphous systems. Such localization is due to the nanometric thickness of the well layers [see the trend in Fig. 1(a)] and to the presence of the barrier layers which prevents carrier diffusion among the various well layers. Such a statement is confirmed by the spectra shown in Fig. 1(b). In fact, the PL intensity decreases as the barrier thickness decreases. When tunneling between well layers through the barrier layers is possible, the spatial confinement of carriers in the well is no longer effective, and an escape mechanism exists which reduces the radiative recombination.

On the other hand, the blueshift could be explained by a quantum confinement effect. Within the effective-mass

theory and assuming infinite potential barriers, the energy gap $E_{04}(d_w)$ for bidimensionally confined $a\text{-Si}_{0.6}\text{N}_{0.4}:\text{H}$ should vary as

$$E_{04}(d_w) = E_{04}^{\text{bulk}} + \frac{\pi^2 \hbar^2}{2d_w^2} \left(\frac{1}{m_e^*} + \frac{1}{m_h^*} \right) \quad (1)$$

where m_e^* and m_h^* are the electron and hole effective masses, and d_w is the well thickness.

Following the model of Dunstain and Boulitrop,¹³ the luminescence process in amorphous semiconductors is due to the recombination of hole-electron pairs that thermalize into the deepest band-tail states distributed randomly in space but exponentially in energy within a critical volume. The critical volume depends on the Street's critical radius¹³ for nonradiative tunneling, and on the slope of the conduction- and valence-band tails. This model yields a fairly linear dependence of the Stokes shift ($E_{04} - E_L$) between energy gap E_{04} and the luminescence energy E_L on the broadest band-tail slope, and is experimentally verified for $a\text{-SiN}$ alloys,^{14,15}

$$E_{04} - E_L = a + bE_U, \quad (2)$$

where a and b are constants which mainly depends on the critical radius, and E_U is the Urbach energy. cw PL and PDS measurements performed on a large number of homogeneous $a\text{-Si}_{1-x}\text{N}_x:\text{H}$ films, with x ranging from 0.15 to 0.52, yield a best linear fit with $a = 0.56 \pm 0.06$ eV and $b = 3.11 \pm 0.40$.¹⁵

From Eqs. (1) and (2) it follows that

$$E_L(d_w) = E_{04}^{\text{bulk}} + \frac{\pi^2 \hbar^2}{2d_w^2} \left(\frac{1}{m_e^*} + \frac{1}{m_h^*} \right) - a - bE_U(d_w). \quad (3)$$

If we consider a linear increase of E_U as d_w decreases,¹⁶ due to an enhancement of the structural disorder, and if $m_e^* = 0.2m_0$ and $m_h^* = 1.0m_0$,¹⁷ a good agreement between the PL blueshift predicted by Eq. (3) and the experimental data is found, as shown by the inset in Fig. 1(a).

In the case of thin barriers, no true bidimensional confinement occurs, and Eq. (3) is no longer valid. A "superlattice" effect settles in with tunneling of carriers between nearby wells and, consequently, a lower-energy confinement. In this case, the absence of a blueshift for the sample with 10-Å-thick wells and barriers shown in Fig. 1(b) could be attributed to a low carrier confinement. Recombination in the gap states of the barrier layers should not be excluded as a concurrent reason.

Another striking result of Fig. 1 is the absence of the PL quenching which was observed by other authors when the well thickness is lower than few tens of Å.¹⁰ This effect was ascribed to a large density of nonradiative recombination centers present at the well/barrier heterointerfaces. To check this, we performed PDS measurements on thick alloy samples whose composition is equal to that of the well layer material. By comparing the results for a 7500-Å-thick sample, where bulk defects predominate, with those for a 450-Å-thick sample, where defects present at the air-film and film-substrate interfaces predominate,¹⁸ an increase of one order of magnitude in the low-energy absorption is measured (see Fig. 2). Interestingly, a 25-period multilayer sample shows an absorption almost equal to the 450-Å-thick sample, whose thickness is comparable to that of a multilayer. This

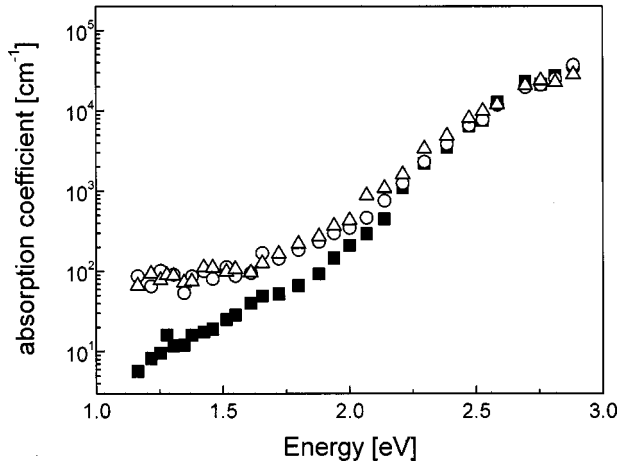


FIG. 2. Absorption coefficient for a 7500-Å-thick *a*-Si_{0.6}N_{0.4}:H film (■ symbols), 450-Å-thick *a*-Si_{0.6}N_{0.4}:H film (● symbols), and a multilayer sample with 25 periods of 10-Å-wide barrier and well layers (△ symbols).

fact indicates that no additional optically active defects have been introduced in the multilayer structure by the presence of the multiple barrier/well heterointerfaces. These observations explain the absence of the PL quenching for the very thin well layers in our samples.

The PDS spectra of Fig. 2 yield a similar value of Urbach energy for both homogeneous and multilayer samples, that would seem to contradict the above assumptions concerning the disorder enhancement in multilayer structure with very thin well layers. On the other hand, it is worth underlining that the Urbach parameter E_U , related to the disorder, can be different for optical and recombination processes. In detail, absorption is sensitive only to antiparallel potential fluctuations, while in a recombination process involving thermalization the carriers interact with states related both to parallel and antiparallel fluctuations.¹⁹ Thus, the broadening of the electronic density of states that influences the photoluminescence process could be underestimated by absorption characterizations.

Figure 3 shows the PL decays for a reference bulk *a*-Si_{0.6}N_{0.4}:H sample [Fig. 3(a)] and for a 30-period *a*-Si_{0.6}N_{0.4}:H/*a*-Si₃N₄:H multilayer structure [Fig. 3(b)] at several emission energies E_{em} . As the detection energy increases, the decay time shortens. To exclude any contributions of direct recombinations in the barrier layer, a thick *a*-Si₃N₄:H film was also investigated. Within the sensitivity of our instrumentation, no PL was measured. Very short decays are observed both for the reference bulk *a*-Si_{0.6}N_{0.4}:H sample and for the multilayer. The decay line shapes do not follow single or double exponential laws, as reported in Ref. 6, but a stretched-exponential law. The mathematical expression of the stretched exponential is

$$I(t) = I_0 \exp[-(t/\tau)^\beta], \quad (4)$$

where $I(t)$ is the luminescence intensity at time t , τ is the decay lifetime, and β is a dispersion exponent. Short $\tau \approx 0.01$ – 0.2 ns and small $\beta \approx 0.3$ – 0.4 are deduced by least-square fits of the decay data. To discuss the experimental data, we consider the PL intensity $I(t)$ to be composed of an

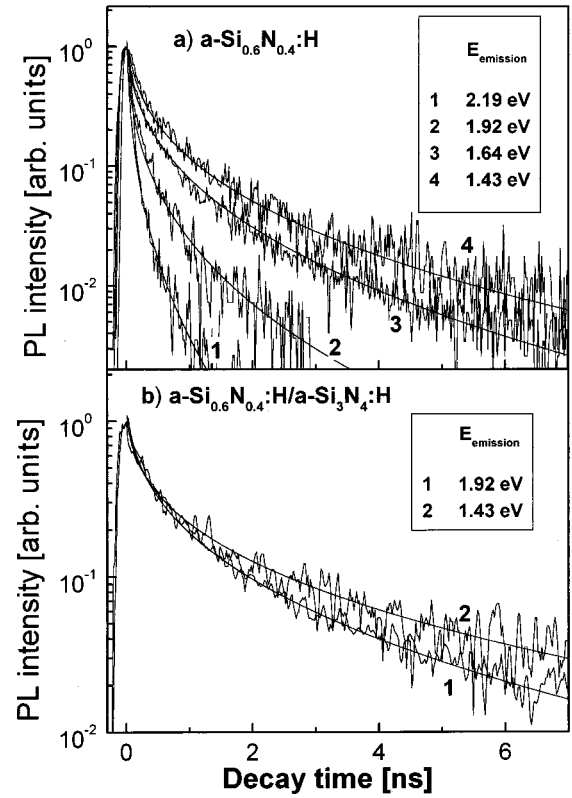


FIG. 3. Time-resolved photoluminescence at room temperature for (a) an *a*-Si_{0.6}N_{0.4}:H film, and (b) an *a*-Si_{0.6}N_{0.4}:H/*a*-Si₃N₄:H multilayer ($d_w = 10$ Å, $d_b = 100$ Å). The spectra at several emission energy are reported. The smooth curves show the results of the best fit using the stretched-exponential function.

infinite number of pure exponentials weighted by a decay rate distribution $G(\tau)/\tau$ (Ref. 20):

$$I(t) = \text{const} \int_0^\infty \frac{G(\tau)}{\tau} \exp\left(-\frac{t}{\tau}\right) d\tau. \quad (5)$$

Extracting the β and τ parameters of Eq. (4) by least-square fits, an asymptotic function has been used to estimate the distribution $G(\tau)$,²¹ and the average decay time was defined as

$$\bar{\tau} = \frac{\int_0^\infty \tau G(\tau) d\tau}{\int_0^\infty G(\tau) d\tau}. \quad (6)$$

In Fig. 4, $\bar{\tau}$ is plotted versus E_{em} for a multilayer structure (30 periods of *a*-Si_{0.6}N_{0.4}:H/*a*-Si₃N₄:H, $d_w = 10$ Å, and $d_b = 100$ Å) and two homogeneous *a*-Si_{1-x}N_x:H alloys (*a*-Si_{0.6}N_{0.4}:H and *a*-SiN:H samples with an emission band at the same energy as the multilayer). Smaller $\bar{\tau}$ values are measured for the alloys than for the multilayer. An exponential dependence $\bar{\tau} \propto \exp(-E/\gamma)$ fits the experimental data with higher γ for *a*-Si_{1-x}N_x:H alloys with a high N content.

Such a dependence could be accounted for by a dominant hopping process through which photogenerated carriers thermalize in lower-energy tail states. Hopping opens an escape mechanism which acts to reduce the recombination lifetime.

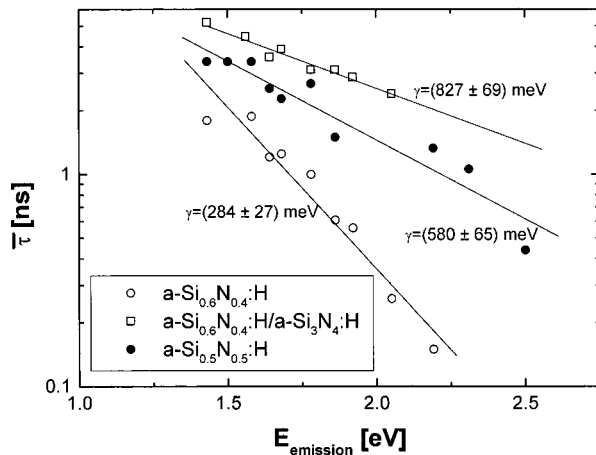


FIG. 4. Average decay time vs detection energy for $a\text{-Si}_{0.6}\text{N}_{0.4}\text{:H}$ and $a\text{-Si}_{0.5}\text{N}_{0.5}\text{:H}$ films and for an $a\text{-Si}_{0.6}\text{N}_{0.4}\text{:H}/a\text{-Si}_3\text{N}_4\text{:H}$ multilayer ($d_w = 10 \text{ \AA}$, $d_b = 100 \text{ \AA}$). The respective γ values yielded by the best exponential fits are indicated.

The hopping rate is proportional to the density of localized states which are involved in the thermalization.²² Moreover, due to the static disorder, $a\text{-Si}_{1-x}\text{N}_x\text{:H}$ alloys are characterized by a density of states (DOS) which shows exponential band tails at the band edges. γ will depend on the slope of the exponential DOS: a sharper DOS profile leads to a smaller γ . In $a\text{-SiN:H}$ the exponential slope of the DOS is a decreasing function of N content, and the DOS extent is larger for N-rich alloys.²³ These facts help to understand the N content and energy dependencies of $\bar{\tau}$. When the same energy interval is observed for the emission of $a\text{-SiN:H}$ alloys, by increasing the N content one expects and, indeed, measures (i) a larger $\bar{\tau}$ due to the lower tail DOS, and (ii) a higher γ due to a lower slope of the exponential DOS. The high decay times and the weak energy dependence of $\bar{\tau}$ for multilayers, compared to alloys, can be explained by the same arguments taking into account a widening of tail states in the well layers due to static disorder and to a decrease of edge states.⁹ It has to be pointed out that $\bar{\tau}$ is just the average of the effective lifetime distribution. On the other hand, if we use a single exponential fit $\exp(-t/\tau_1)$ to $I(t)$ for $0 \leq t \leq 1 \text{ ns}$, a more smooth energy dependence of τ_1 with respect to $\bar{\tau}$ is found for Si-rich $a\text{-Si}_{1-x}\text{N}_x\text{:H}$ alloys, while almost no energy dependence is measured for N-rich $a\text{-Si}_{1-x}\text{N}_x\text{:H}$ or multilayer samples. The above results suggest that the

thermalization process affects mainly the decay rate at $t > 1 \text{ ns}$. Measurement performed as a function of the temperature should allow a discrimination of various contributions to the luminescence decay.

No dependence of the decay line shape on the excitation intensities (ranging from $5\text{--}5 \times 10^2 \mu\text{W}$ of average power) is observed. Furthermore, there is a linear dependence of the PL intensity on the excitation intensity. This signs a monomolecular recombination regime that is observed even at room temperature in this work. This has already been observed in C-rich $a\text{-SiC:H}$ alloys, and was justified by the strong electron-hole Coulomb interaction.¹⁹ Similarly, in $a\text{-Si}_{1-x}\text{N}_x\text{:H}$ -based alloys and multilayers, an enhancement of the Coulomb interaction by increasing the nitrogen content is possible due to a decrease of the refractive index.⁵

It is worth emphasizing that a comparison of the photoluminescence spectra of the multilayers excited with photons of 2.71 eV (the cw PL measurements) with those excited with photons of 3.2 eV (both time-integrated and spectrally resolved TRL measurements) does not exhibit any appreciable energy shift between the spectral features. Such a behavior seems to exclude the fact that the strong enhancement in the PL efficiency observed for multilayer structures is due to the partial intermixing of the barrier and well layers with the formation of a N-rich $a\text{-Si}_{1-x}\text{N}_x\text{:H}$ layer at the heterointerfaces.¹⁷ In such a case, a blueshift of the PL emission would be observed by varying the excitation energy from 2.71 to 3.2 eV, as found in $a\text{-Si}_{1-x}\text{N}_x\text{:H}$ alloys excited at energies below the gap energy.²³

In conclusion, the optical measurements performed on $a\text{-Si}_{1-x}\text{N}_x\text{:H}$ -based nanometric multilayers show (i) room-temperature fast monomolecular emission with high efficiencies due to the spatial localization of carriers in the narrow well layers, which seems compatible with carrier confinement associated with a disorder enhancement; (ii) a low heterointerface defect concentration and an absence of interface intermixing; and (iii) a recombination dynamic dominated at room temperature by hopping that induces, more markedly for Si-rich $a\text{-SiN}$ than for multilayers, a dependence of the decay times on the emission energy. In the light of such results, wide-band-gap $a\text{-Si}_{1-x}\text{N}_x\text{:H}$ -based multilayer structures open the possibility of applications in optoelectronic devices, such as fast light-emitting devices with high brightnesses in the visible range.

The authors wish to thank Dr. P. Rava for samples deposition and the LAMEL-CNR Institute, where the multichamber PECVD system is located.

*Author to whom correspondence should be addressed. Electronic address: giorgis@polito.it

¹S. Miyazaki, N. Murayama, and M. Hirose, *J. Non-Cryst. Solids* **77–78**, 1089 (1985).

²M. Tsukude, S. Akamatsu, S. Miyazaky, and M. Hirose, *Jpn. J. Appl. Phys.* **26**, L111 (1987).

³S. Miyazaky and M. Hirose, in *Amorphous and Microcrystalline Semiconductor Devices: Optoelectronic Devices*, edited by J. Kanicki (Artech House, Boston, 1991), Vol. 1, p. 167.

⁴D. Kruangam, M. Deguchi, T. Endo, H. Okamoto, and Y. Hamakawa, in *Amorphous Silicon Semiconductors—Pure And Hy-*

drogenated, edited by A. Madau, M. Thompson, D. Adler, and Y. Hamakawa, MRS Symposium Proceedings No. 95 (Materials Research Society, Pittsburgh, 1987) p. 609.

⁵F. Giorgis, C. F. Pirri, and E. Tresso, *Thin Solid Films* **307**, 298 (1997).

⁶S. V. Deshpande, E. Gulari, S. W. Brown, and S. C. Rand, *J. Appl. Phys.* **77**, 6534 (1995).

⁷A. Madan, P. Rava, R. E. I. Schropp, and B. Von Roedern, *Appl. Surf. Sci.* **70–71**, 216 (1993).

⁸F. Giorgis, F. Giuliani, C. F. Pirri, E. Tresso, R. Galloni, R. Rizoli, C. Summonte, A. Desalvo, F. Zignani, P. Rava, and F.

- Caccavale, in *Title*, edited by Editor(s), MRS Symposia, Proceedings No. 467 (Materials Research Society, Pittsburgh, 1997), p. 489.
- ⁹T. Tiedje, B. Abeles, and B. G. Brooks, *Phys. Rev. Lett.* **54**, 2545 (1985).
- ¹⁰W. C. Wang and H. Fritzsche, *J. Non-Cryst. Solids* **97&98**, 919 (1987).
- ¹¹Chun Gen, V. Yu. Kaznacheev, and A. E. Yunovich, *Fiz. Tekh. Poluprovodn.* **25**, 1681 (1991) [*Sov. Phys. Semicond.* **25**, 1011 (1991)].
- ¹²G. Allan, C. Dellerue, and M. Lannoo, *Appl. Phys. Lett.* **71**, 1189 (1997).
- ¹³F. Boulitrop and D. J. Dunstain, *Phys. Rev. B* **28**, 5923 (1983).
- ¹⁴T. M. Searle and W. A. Jackson, *Philos. Mag. B* **60**, 237 (1989).
- ¹⁵F. Giorgis (unpublished).
- ¹⁶For the calculation, a linear enhancement of E_U as d_w decreases has been considered, starting from $E_U(d_w=20 \text{ \AA})=144 \text{ meV}$, the same value measured for the reference bulk sample, up to $E_U(d_w=5 \text{ \AA})=200 \text{ meV}$, which is the only free parameter in the fit of $E_L(d_w)$.
- ¹⁷S. Kalem, *Phys. Rev. B* **37**, 8837 (1988).
- ¹⁸G. Amato, F. Giorgis, and C. Manfredotti, in *Amorphous Silicon Technology—1993*, edited by E. A. Schiff, M. J. Thompson, A. Madan, K. Tanaka, and P. G. LeComber, MRS Symposia Proceedings No. 297 (Materials Research Society, Pittsburgh, 1993), p. 389.
- ¹⁹L. R. Tessler and I. Solomon, *Phys. Rev. B* **52**, 10962 (1995).
- ²⁰K. Suzuki, G. Bley, V. Neukirch, J. Gutoski, N. Takojima, T. Sawada, and K. Imai, *Solid State Commun.* **105**, 571 (1998).
- ²¹S. Sawada, N. Hamada, and N. Ookubo, *Phys. Rev. B* **49**, 5236 (1994).
- ²²S. Kivelson and C. D. Gelatt, Jr., *Phys. Rev. B* **26**, 4646 (1982).
- ²³I. G. Austin, W. A. Jackson, T. M. Searle, P. K. Bhat, and R. A. Gibson, *Philos. Mag. B* **52**, 271 (1985).